

# Differential expression analysis for sequence count data

Simon Anders\*, Wolfgang Huber

European Molecular Biology Laboratory (EMBL), Heidelberg, Germany

7 Jan 2010

## Abstract

**Motivation:** High throughput nucleotide sequencing provides quantitative readouts in assays for RNA expression (RNA-Seq), protein-DNA binding (ChIP-Seq), cell counting. Statistical inference of differential signal in these data needs to take into account their natural variability throughout the dynamic range. When the number of replicates is small, error modeling is needed to achieve statistical power.

**Results:** We propose an error model that uses the negative binomial distribution, with variance and mean linked by local regression, to model the null distribution of the count data. The method controls type I error and provides good detection power.

**Availability:** A free open-source R software package, called *DESeq*, is available from <http://www.huber.embl.de/users/anders/DESeq> (and will be available from the Bioconductor project).

**Contact:** sanders@fs.tum.de

## 1 Introduction

High-throughput sequencing of DNA fragments offers unprecedented opportunities for the monitoring of RNA abundance and of protein-DNA binding, including the possibility to discover novel sequence variants and to dissect allele-specific effects and genetic variation. There is a range of technologies; a common feature between them is that they produce large amounts of sequence reads sampled from a preparation of DNA fragments that reflects, e.g., a biological system's repertoire of RNA molecules (RNA-Seq, Nagalakshmi et al. (2008); Mortazavi et al. (2008)) or the DNA or RNA interaction regions of nucleotide binding molecules (ChIP-Seq, Robertson et al. (2007); HITS-CLIP, Licatalosi et al. (2008)). Typically, these reads are classified based on their mapping to a common region of the target genome, where each class represents a target transcript, in the case of RNA-Seq, or a binding region, in the case of ChIP-Seq. An im-

portant summary statistic is the number of reads in a class; for RNA-Seq, this *read count* has been found to be (to good approximation) linearly related to the abundance of the target transcript (Mortazavi et al., 2008). Interest lies in comparing read counts between different biological conditions or between different genetic variants. In the simplest case, the comparison is done separately, class by class. We will use the term *gene* synonymously to *class*, even though a class may also refer to, e.g., a transcription factor binding site, or even a barcode (Smith et al., 2009).

We would like to use statistical testing to decide whether, for a given gene, an observed difference in read counts is significant, i.e., whether it is greater than what would be expected just due to natural random variation.

If reads are independently sampled from a population with given, fixed fractions of genes, the read counts follow a multinomial distribution, which can be approximated by Poisson distributions. Consequently, Poisson distributions have been used to test for differential expression (Marioni et al., 2008; Wang et al., 2010). The single parameter of a Poisson distribution is determined by its mean, and its variance and all other properties follow from that; especially, the variance is equal to the mean. However, it has been noted (Robinson and Smyth, 2007; Nagalakshmi et al., 2008) that the assumption of Poisson distribution for the read counts is too tight, i.e., it predicts smaller variations than what is seen in the data. The resulting statistical test does therefore not control the type I error (the probability of false discoveries) as advertised. We show instances for that in Section 5.1.

To address this so-called overdispersion problem, it has been proposed to model count data with negative binomial (NB) distributions (Whitaker, 1914), and this approach is used in the *edgeR* package for analysis of SAGE and RNA-Seq (Robinson and Smyth, 2007; Robinson et al., 2010). The NB distributions are a family with two parameters, which are uniquely determined by mean  $\mu$  and variance  $v$ . However, the number of replicates in datasets of interest is often too small to estimate both of those two parameters, mean

---

\*sanders@fs.tum.de

and variance, reliably for each gene. For *edgeR*, Robinson and Smyth (2008) proposed to assume that mean and variance are related by  $v = \mu + \alpha\mu^2$ , with a single proportionality constant  $\alpha$  that is the same throughout the experiment and that can be readily estimated from the data. Hence, only one parameter needs to be estimated for each gene, allowing application to experiments with small numbers of replicates.

In this paper, we extend this model by allowing more general, data-driven relationships of variance and mean, provide an effective algorithm for fitting the model to data, and show that it provides better fits. As a result, more balanced selection of differentially expressed genes throughout the dynamic range of the data and higher power for the detection of differential abundance can be obtained. The method is applicable to a wide range of experimental designs and questions.

We will first specify our model and explain how to fit its parameters (Section 2) and then how to test for differential expression (Section 3). We demonstrate the method by applying it to three data sets (Section 4) and discuss how it compares to alternative approaches (Section 5). Finally, we present the R implementation of the method, called *DESeq* (Section 6).

## 2 Model

### 2.1 Description

We assume that the number of reads in sample  $j$  that are assigned to gene  $i$  can be modeled by a negative binomial (NB) distribution,

$$K_{ij} \sim \text{NB}(\mu_{ij}, \sigma_{ij}^2), \quad (1)$$

which has two parameters, the mean  $\mu_{ij}$  and the variance  $\sigma_{ij}^2$ . The read counts  $K_{ij}$  are non-negative integers. The probabilities of the distribution are given in Supplementary Note A. This family of distributions is commonly used to model count data when overdispersion is present (Cameron and Trivedi, 1998).

In practice, we do not know the parameters  $\mu_{ij}$  and  $\sigma_{ij}^2$ , and we need to fit them from the data. Typically, the number of replicates is small, and further modeling assumptions need to be made in order to obtain useful estimates. In this paper, we develop a method that is based on the following three assumptions:

First, the mean parameter  $\mu_{ij}$ , that is, the expectation value of the observed counts for gene  $i$  in sample  $j$ , is the product of a condition-dependent per-gene value  $q_{i,\rho(j)}$  (where  $\rho(j)$  is the experimental condition of sample  $j$ ) and a library size parameter  $s_j$ ,

$$\mu_{ij} = q_{i,\rho(j)} s_j. \quad (2)$$

$q_{i,\rho(j)}$  is proportional to the expectation value of the true (but unknown) concentration of fragments from gene  $i$  under condition  $\rho(j)$ . The library size parameter  $s_j$  is proportional to the coverage, or sampling depth, of library  $j$ , and we will use the term common scale for quantities, such as  $q_{i,\rho(j)}$ , that are adjusted for coverage by dividing by  $s_j$ .

Second, the variance  $\sigma_{ij}^2$  is the sum of a *shot noise term* and a *raw variance term*,

$$\sigma_{ij}^2 = \underbrace{\mu_{ij}}_{\text{shot noise}} + \underbrace{s_j^2 v_{i,\rho(j)}}_{\text{raw variance}} \quad (3)$$

Third, the per-gene raw variance parameter  $v_{i,\rho(j)}$  is a smooth function  $v_\rho$  of the per-gene abundance  $q_{i,\rho(j)}$ ,

$$v_{i,\rho(j)} = v_\rho(q_{i,\rho(j)}). \quad (4)$$

The decomposition of the variance in Equation (3) is motivated by the following hierarchical model. We assume that the actual concentration of fragments from gene  $i$  in sample  $j$  is proportional to a random variable  $R_{ij}$ , such that the rate that fragments from gene  $i$  are actually sequenced is  $s_j r_{ij}$ . For each gene  $i$  and all samples  $j$  of condition  $\rho$ , the  $R_{ij}$  are i.i.d. with mean  $q_{i\rho}$  and variance  $v_{i\rho}$ . Thus, the count value  $K_{ij}$ , conditioned on  $R_{ij} = r_{ij}$ , is Poisson distributed with rate  $s_j r_{ij}$ . If the higher moments of the distribution of  $R_{ij}$  are modeled according to a gamma distribution, the marginal distribution of  $K_{ij}$  is NB (see e.g. Cameron and Trivedi (1998, Sec. 4.2.2)) with mean  $\mu_{ij}$  and variance as given in Equation (3).

The model could be refined by adding further parameters. For example, when the experimental protocols involves DNA fragmentation, one may want to divide the mean  $q_{i\rho}$  in Equation (4) by the feature length.

### 2.2 Fitting

We now describe how the model can be fit to data. The data are an  $n \times m$  table of counts,  $k_{ij}$ , where  $i = 1, \dots, n$  indexes the genes, and  $j = 1, \dots, m$  indexes the samples. The model has three sets of parameters:

1.  $m$  library size parameters  $s_j$ ; the expectation values of all counts from sample  $j$  are proportional to  $s_j$ .
2. for each experimental condition  $\rho$ ,  $n$  gene abundance parameters  $q_{i\rho}$ ; they reflect the expected abundance of fragments from gene  $i$  under condition  $\rho$ , i.e., expectation values of counts for gene  $i$  are proportional to  $q_{i\rho}$ .
3. The smooth functions  $v_\rho : \mathbb{R}^+ \rightarrow \mathbb{R}^+$ ; they model the dependence of the raw variance  $v_{i\rho}$  on the expected mean  $q_{i\rho}$ .

To estimate the size parameters, we use

$$\hat{s}_j = \text{median}_i \frac{k_{ij}}{(\prod_{\nu=1}^m k_{i\nu})^{1/m}}. \quad (5)$$

The denominator of this expression can be interpreted as a pseudo-reference sample obtained by taking the geometric mean across samples. Each library size parameter estimate  $\hat{s}_j$  is then computed as the median of the ratios of the  $j$ -th sample's counts to those of the pseudo-reference. In many cases, the values  $\hat{s}_j$  will be proportional to, and thus equivalent to, the sums  $\sum_i k_{ij}$ . However, it is not uncommon for the sums to be dominated by the counts for a few, highly abundant genes. In such cases, the estimator (5) will be more robust, and will produce a better library size adjustment for the majority of genes.

To estimate  $q_{i\rho}$ , we use the average of the counts from the samples  $j$  corresponding to condition  $\rho$ , transformed to the common scale:

$$\hat{q}_{i\rho} = \frac{1}{m_\rho} \sum_{j:\rho(j)=\rho} \frac{k_{ij}}{\hat{s}_j}, \quad (6)$$

where  $m_\rho$  is the number of replicates of condition  $\rho$  and the sum runs over these replicates.

To estimate the functions  $v_\rho$ , we first calculate sample variances on the common scale

$$w_{i\rho} = \frac{1}{m_\rho - 1} \sum_{j:\rho(j)=\rho} \left( \frac{k_{ij}}{\hat{s}_j} - \hat{q}_{i\rho} \right)^2 \quad (7)$$

and define

$$z_{i\rho} = \frac{\hat{q}_{i\rho}}{m_\rho} \sum_{j:\rho(j)=\rho} \frac{1}{\hat{s}_j}. \quad (8)$$

In Supplementary Note B, we show that  $w_{i\rho} - z_{i\rho}$  is an unbiased estimator for the raw variance parameter  $v_{i\rho}$  of Equation (3).

However, for small numbers of replicates,  $m_\rho$ , as is typically the case in applications, the values  $w_{i\rho}$  are highly variable, and  $w_{i\rho} - z_{i\rho}$  would not be a useful variance estimator for statistical inference. Instead, we use local regression (Loader, 1999) on the graph  $(\hat{q}_{i\rho}, w_{i\rho})$  to obtain a smooth function  $w_\rho(q)$ , with

$$\hat{v}_\rho(\hat{q}_{i\rho}) = w_\rho(\hat{q}_{i\rho}) - z_{i\rho} \quad (9)$$

as our estimate for the raw variance.

Some attention is needed to avoid estimation biases in the local regression.  $w_{i\rho}$  is a sum of squared random variables, and the residuals  $w_{i\rho} - w(\hat{q}_{i\rho})$  do not follow a normal distribution. Following McCullagh and Nelder (1989, Ch. 8) and Loader (1999, Section 9.1.2), we use a generalised linear model of the gamma family for the local regression, using the implementation in the *locfit* package (Loader, 2007).

### 3 Testing for differential expression

Suppose that we have  $m_A$  replicate samples for biological condition A and  $m_B$  samples for condition B. For each gene  $i$ , we would like to weigh the evidence in the data for or against differential abundance of that gene between the two conditions. In particular, we would like to test the null hypothesis  $q_{iA} = q_{iB}$ , where  $q_{iA}$  is the gene abundance parameter for the samples of condition A, and  $q_{iB}$  for condition B. To this end, we define, as test statistic, the total counts in each condition,

$$K_{iA} = \sum_{j:\rho(j)=A} K_{ij} \quad K_{iB} = \sum_{j:\rho(j)=B} K_{ij}, \quad (10)$$

and their overall sum  $K_{iS} = K_{iA} + K_{iB}$ . From the error model of Section 2, we show below that we can compute the probabilities of the events  $K_{iA} = a$  and  $K_{iB} = b$  for any pair of numbers  $a$  and  $b$ . We denote this probability by  $p(a, b)$ . The  $p$ -value of a pair of observed count sums  $(k_{iA}, k_{iB})$  is then the sum of all probabilities less or equal to  $p(k_{iA}, k_{iB})$ , given that the overall sum is  $k_{iS}$ :

$$p_i = \frac{\sum_{\substack{a+b=k_{iS} \\ p(a,b) \leq p(k_{iA}, k_{iB})}} p(a, b)}{\sum_{a+b=k_{iS}} p(a, b)} \quad (11)$$

The variables  $a$  and  $b$  in the above sums take the values  $0, \dots, k_{iS}$ . The approach presented so far follows that of Robinson and Smyth (2008) and is analogous to that taken by other conditioned tests, such as Fisher's exact test. (See Agresti (2002, Ch. 2) for a discussion of the merits of conditioning in tests.)

**Computation of  $p(a, b)$ .** First, assume that, under the null hypothesis, counts from different samples are independent. Then,  $p(a, b) = \Pr(K_{iA} = a) \Pr(K_{iB} = b)$ . The problem thus is computing the probability of the event  $K_{iA} = a$ , and, analogously, of  $K_{iB} = b$ . The random variable  $K_{iA}$  is the sum of  $m_A$  NB-distributed random variables. We approximate its distribution by a NB distribution whose parameters we obtain from those of the  $K_{ij}$ . To this end, we first compute the pooled mean estimate from the counts of both conditions,

$$\hat{q}_{i0} = \sum_{j:\rho(j) \in \{A, B\}} k_{ij} / s_j, \quad (12)$$

which accounts for the fact that the null hypothesis stipulates that  $q_{iA} = q_{iB}$ . The summed mean and

variance for condition A is

$$\hat{\mu}_{iA} = \sum_{j \in A} s_j \hat{q}_{i0}, \quad (13)$$

$$\hat{\sigma}_{iA}^2 = \sum_{j \in A} \hat{s}_j \hat{q}_{i0} + \hat{s}_j^2 \hat{v}_A(\hat{q}_{i0}), \quad (14)$$

Supplementary Note C describes how the distribution parameters of the NB for  $K_{iA}$  can be determined from  $\hat{\mu}_{iA}$  and  $\hat{\sigma}_{iA}^2$ . (We do not use the moments directly but instead perform an additional bias-correcting step.) The parameters of  $K_{iB}$  are estimated analogously. Supplementary Note D explains how we evaluate the sums in Equation (11).

## 4 Applications

### 4.1 Data sets

We demonstrate the application of our method, which we call *DESeq*, on the following data sets.

**Tag-Seq of neural stem cells.** Engström et al. (2010) performed Tag-Seq (Morrissy et al., 2009) for tissue cultures of neural cells, including two from glioblastoma-derived neural stem-cells (condition *GNS*; samples G144, G166) and two from non-cancerous neural stem cells (condition *NS*; samples NS123, NS345). The number of reads obtained from each library varied from 7.6 millions to 13.6 millions. A good fraction of these (depending on the sample, from 32% to 53%) could be unambiguously assigned to annotated genes, and Engström et al. (2010) et al. summarised the data in a table of counts with six columns for the six samples and 18,760 rows, one for each gene.

**RNA-Seq of yeast.** Nagalakshmi et al. (2008) performed RNA-Seq on replicates of yeast cultures. They tested two library preparation protocols, *dT* and *RH*, and obtained three sequencing runs for each protocol, such that for the first run of each protocol, they had one further technical replicate (same culture, replicated library preparation) and one further biological replicate (different culture).

**ChIP-Seq in humans.** This dataset contains four replicates each from a ChIP-Seq experiment studying polymerase-II occupancy in two different human individuals.

### 4.2 Variance estimation

We start by demonstrating the variance estimation. Figure 1a shows the sample variances  $w_{i\rho}$  (Equation (7)) plotted against the means  $\hat{q}_{i\rho}$  (Equation (6))

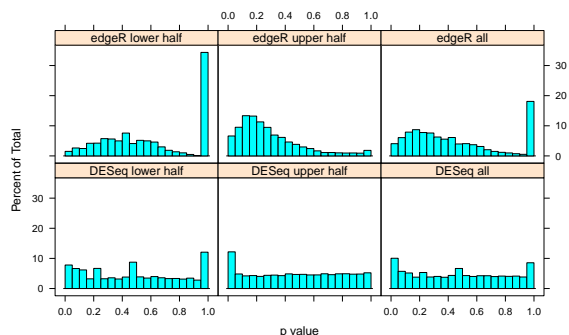


**Figure 3:** Type-I error control. The histograms show  $p$  values from a comparison of one *GNS* replicate with another one. Between replicates, no genes are truly differentially expressed, and the distribution of  $p$ -values is expected to be uniform in the interval  $[0, 1]$ . Top row shows results for *edgeR*, lower row for *DESeq*. Left and middle column show the distributions separately for genes below and above the median mean, right column for all genes. *DESeq*'s more flexible variance estimation leads to approximately uniform  $p$  value distributions independent of the mean level, whereas those obtained with *edgeR* show intensity dependent trends.

for the condition  $\rho = \text{GNS}$  in the neural stem cells data. Also shown is the local regression fit  $w_\rho(q)$  and the shot noise  $\hat{s}_j \hat{q}_{i\rho}$ . In Figure 1b, we plotted the squared coefficient of variation (SCV), i.e. the ratio of the variance to the mean squared. In this plot, the distance between the orange and the purple line is the SCV of the noise due to biological sampling (cf. Equation (3)).

The many points in Figure 1a that lie far above the fitted orange curve may let the fit of the local regression appear poor. However, a strong skew of the residual distribution is to be expected. See Supplementary Note E for details and a discussion of diagnostics suitable to verify the fit.

### 4.3 Testing

In order to verify control of type-I error, we contrasted one *GNS* replicate against another replicate of the same condition, using for both samples the variance function estimated for condition *GNS*. In this case, we expect to find uniformly distributed  $p$  values. Figure 3 (lower row) shows this to be the case.

Next, we contrasted the two *GNS* samples against the two *NS* samples. Using the procedure described in Section 3, we computed a  $p$  value for each gene. Figure 2 shows the obtained fold changes and  $p$  values. 10% of the  $p$  values are below 5%. Adjustment for multiple-testing with the false discovery rate (FDR) controlling procedure of Benjamini and Hochberg (1995) yielded significant differential expres-

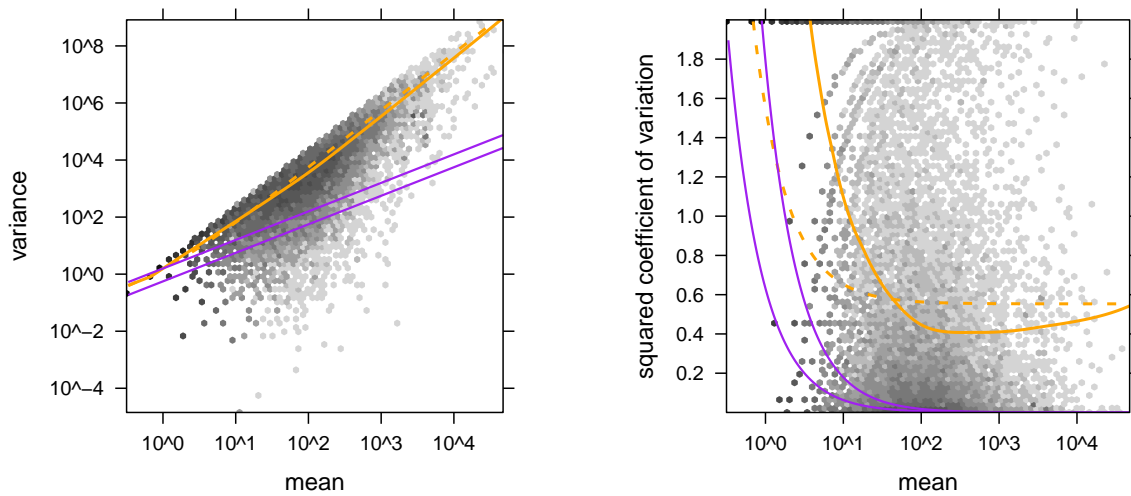


**Figure 1:** Dependence of the variance on the mean for the two *GNS* samples from the neural stem cells data. (a) The scatter plot shows the common-scale sample variances (Equation (7)) plotted against the common-scale means (Equation (6)). The orange line is the fit  $w(q)$ . The purple lines show the variance implied by the Poisson distribution for each of the two *GNS* samples, i.e.,  $\hat{s}_j \hat{q}_{i,GNS}$ . The dashed orange line is the variance estimate used by *edgeR*. (b) Same data as in (a), with the *y*-axis rescaled to show the squared coefficient of variation (SCV), i.e. all quantities are divided by the square of the mean. The solid orange line is computed using the bias correction described in Supplementary Note C.

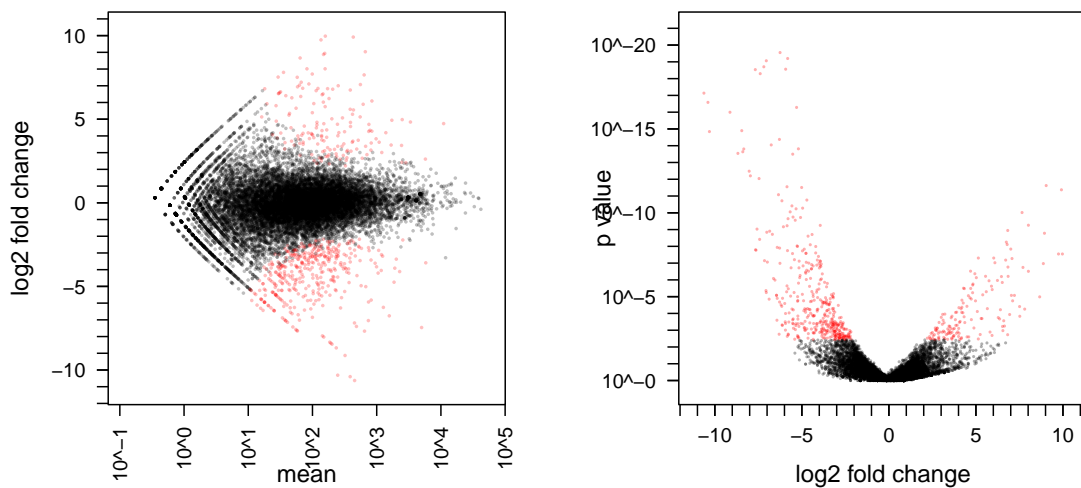


**Figure 2:** Testing for differential expression between conditions *GNS* and *NS*. (a) Scatter plot of  $\log_2$  fold changes versus mean. The red colour marks genes detected as differentially expressed at 10% false discovery rate when the Benjamini-Hochberg multiple testing adjustment is used. (b) Volcano plot.

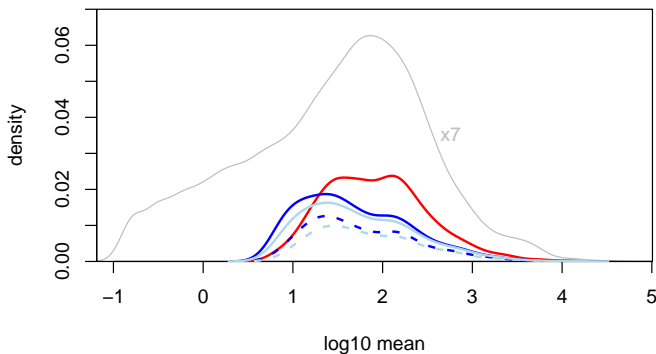


**Figure 4:** The density of common-scale mean values  $q_i$  for all genes (grey line, scaled down by a factor of 7, for the hits reported by *DESeq* (red line) and by *edgeR* with four different settings (light blue, using read count sum for library size adjustment; dark blue, using Equation (5); solid, with common dispersion; dashed, with tagwise dispersion.)

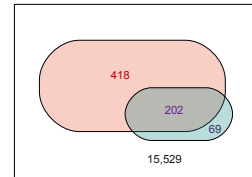
sion at a 10% FDR level for a set of 680 genes (of 18,323). These are marked in red in the figure.

Figure 2 demonstrates that the power to detect differential expression depends on overall counts: below a common scale mean of  $\sim 10$ , no detection is possible, and as the mean grows, smaller fold changes become detectable.

#### 4.4 Comparison with edgeR

We also compared the three *GB* samples with the two *NS* samples using *edgeR* (version 1.5.4; Robinson and Smyth (2007, 2008); Robinson et al. (2010)). While *DESeq* reports 680 genes at Benjamini-Hochberg adjusted FDR of 10%, *edgeR* finds 452 genes when used in *common dispersion* mode and 256 in the *tagwise dispersion* mode. These numbers for *edgeR* were obtained when supplying it with total read counts as library size parameters, as recommended in the documentation; when *DESeq*'s estimates, as in Equation (5), were used, we obtained 525 and 316 genes, respectively. 84% to 96% of *edgeR*'s genes were also reported by *DESeq*, which is consistent with an FDR of 10%.

The difference between the results of *edgeR* and *DESeq* does not merely lie in the number of genes, but also in their properties. As can be seen from Figure 4, the gene lists have different distributions along the abundance scale. While –for these data– *edgeR*'s hits tend to concentrate at lower abundance, the hits from *DESeq* are more evenly distributed along the dy-



**Figure 5:** Calling differential expression without replicates: The red set in this Venn diagram represents the genes that were found to show differential expression significant at 10% FDR when comparing three *GNS* samples with the two *NS* samples. When using only one sample of each type, the genes represented by the blue set are found.

namic range, once the mean is above  $\sim 10$ . *edgeR*'s bias towards lower abundance genes is likely not a reflection of biology, but rather an artifact of its error model: *edgeR* estimates a common dispersion of 0.56 (0.60 with read count sum). The dashed orange line in Figure 1a and b shows the variance implied by a raw SCV of this value. As one can see, it is lower than *DESeq*'s estimate (solid orange line) for the lower part of the dynamic range, and higher in the upper range. Hence, *edgeR* calls more hits among genes with low counts and is conservative for genes with high counts. This matches the observation from Figure 4. On average, over the whole dynamic range, FDR control is of course maintained, albeit at the cost of detection power.

A similar effect can be observed in the comparison of the two *GNS* replicates against each other. As can be seen in Figure 3, there are either too many high or too many low  $p$  values, depending on the range of mean values.

#### 4.5 Working without replicates

*DESeq* allows analysis of experiments with no biological replicates in one or even in both of the conditions. While one may not want to draw strong conclusions from such an analysis, it may still be useful for exploration and hypothesis generation.

If replicates are available only for one of the conditions, one may assume that the variance-mean dependence estimated from the data for that condition holds as well for the unreplicated one.

If neither condition has replicates, one can still perform an analysis based on the assumption that for most genes, there is no true differential abundance, and that a valid mean-variance relationship can be estimated from treating the two samples as if they were replicates. A minority of differentially abundant genes will act as outliers, however, they will not have a severe impact on the gamma-family GLM fit, as the gamma distribution for low values of the shape pa-

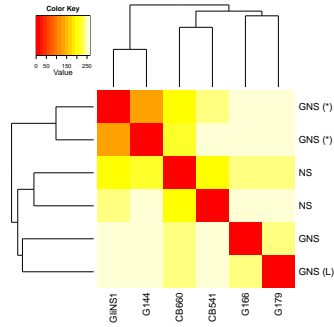


**Figure 6:** Sample clustering for the data of Engström et al. (2010). A common variance function was estimated for all samples and used to apply a variance-stabilizing transformation. The heatmap shows a false colour representation of the Euclidean distance matrix, and the dendrogram represents a hierarchical clustering. The two *GNS* samples derived from the same patient (marked with “(\*)”) show the highest degree of similarity. The two other *GNS* samples (including the one with atypically large cells, marked “(L)”) are as dissimilar from the former as the two *NS* samples.

parameter  $(m - 1)/2$  has a heavy right-hand tail. Some overestimation of the variance may be expected, which will make that approach conservative.

We performed such an analysis by restricting the neural stem cells data to only two samples, one from the *GNS* and one from the *NS* condition. The estimated variance function is, as expected, above the two functions estimated from the *GNS* and *NS* replicates. Using it to test for differential abundance still finds a number of hits at 10% FDR, as can be seen from the Venn diagram in Figure 5, and these hits have good overlap with those found from the more reliable analysis with all available samples.

## 4.6 Variance-stabilizing transformation

Given a variance-mean dependence, a variance-stabilizing transformation (VST) is a bijection such that for the transformed values, the variance is (approximately) independent of the mean. Using the variance-mean dependence estimated by *DESeq*, the function  $v(q)$ , a VST is given by

$$\tau(\kappa) = \int^{\kappa} \frac{dq}{\sqrt{v(q)}}. \quad (15)$$

Using the transformation  $\tau$  on the common-scale count data,  $k_{ij}/s_j$ , yields new data values whose variance is approximately the same throughout the dynamic range.

One application of VST is sample clustering, as in Figure 6; such an approach is more straightforward than, say, defining a suitable distance metric on the

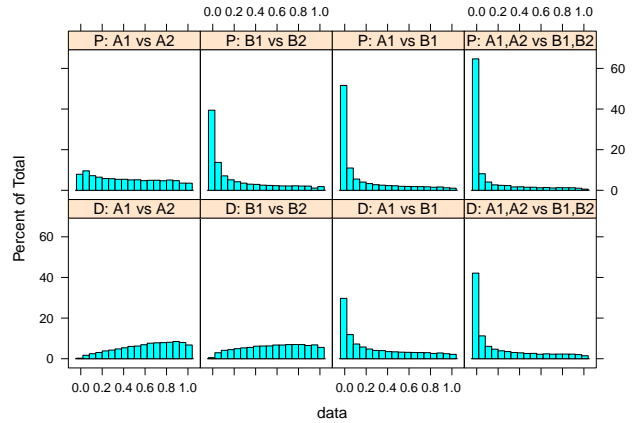


**Figure 7:** Application to ChIP-Seq data. Shown are  $p$  value histograms resulting from comparisons of Pol-II ChIP-Seq data between replicates of the same individual (first and second column) and between two different individuals (third and fourth column). The upper row corresponds to an analysis based on Poisson GLMs (“P”), the bottom row to analysis with *DESeq* (“D”). In the first column, two replicates from individual A (replicate set *A1*) are compared against two further replicates from the same individual (*A2*). As expected, the  $p$  value histograms are approximately flat, indicating no significant differences. In the second column, two replicates from individual B (*B1*) are compared against two further replicates from the same individual (*B2*). While no significant differences are expected, the Poisson GLM analysis finds an enrichment of small  $p$  values; this is a reflection of overdispersion in the data, that is, the variance in the data is larger than what the Poisson GLM assumes (see also Section 5.1). The third column compares two replicates from individual A (*A1*) against two from individual B (*B1*). True binding differences are expected, and both methods result in an excess of small  $p$  values. The fourth column shows the comparison of four replicates of individual A (*A1* combined with *A2*) against four replicates of individual B (*B1*, *B2*); increased sample size leads to higher detection power.

untransformed count data, whose choice is not obvious, and may not be easy to combine with available clustering or classification algorithms. Another use is the computation of more complex contrasts, such as interactions between experimental factors or regression on continuous-valued variables, and analysing the effects as if the data were homoskedastic. However, the power of such an approach would be lower than in the NB-based approach of Section 3, since it ignores the discreteness and skewedness of the count data.

## 4.7 ChIP-Seq

An application of *DESeq* to ChIP-Seq data is shown in Figure 7. For two human individuals (“A” and “B”), four replicates of ChIP-Seq for polymerase-II had been done. Using a pre-compiled list of binding regions, a table of count data can be obtained by counting the number of reads aligned to each binding region (which



now take the place of genes).

In analysing this table, type-I error control was maintained by *DESeq*: the lower left two panels of Figure 7 show approximately uniform  $p$  value histograms for comparisons within the same individual, and no binding region was significant at 10% FDR using Benjamini-Hochberg adjustment. Differential binding was found, however, when contrasting the two individuals, with 6,450 binding regions significant when only two replicates each were used and 9,415 when four replicates were used.

However, if one assumed the read counts to follow Poisson distributions, a standard approach would be to perform count regression, i.e., to use a generalized linear model (GLM) of the Poisson family (Cameron and Trivedi, 1998). The upper row of Figure 7 shows that for this approach an enrichment of small  $p$  values even for comparisons within the same individual, indicating that the variance is underestimated, and literal use of the  $p$  values would hence lead to anticonservative (overly optimistic) calling of differential binding regions.

## 5 Discussion

Why is it necessary to develop new statistical methodology for sequence count data? If large numbers of replicates were available, questions of data distribution could be avoided by using non-parametric methods, such as Wilcoxon and Kruskal-Wallis tests. However, it is desirable (and possible) to consider experiments with smaller numbers of replicates per condition. In order to compare an observed difference with the to be expected random variation, we can employ two sources of information on the size and nature of random variation: first, we can use distribution families, such as normal, Poisson and negative binomial distributions, in order to determine the higher moments, and hence the tail behavior, of statistics for differential abundance, based on observed low order moments such as mean and variance. Second, we can share information between genes, based on the notion that data from different genes follow similar patterns of variability. Here, we have described an instance of such an approach, and we will now discuss the choices we have made.

### 5.1 Distributional family

While for large counts, the normal distributions might provide a good approximation of between replicate variability, this is not the case for lower count values, whose discreteness and skewness mean that probability estimates computed from a normal approximation

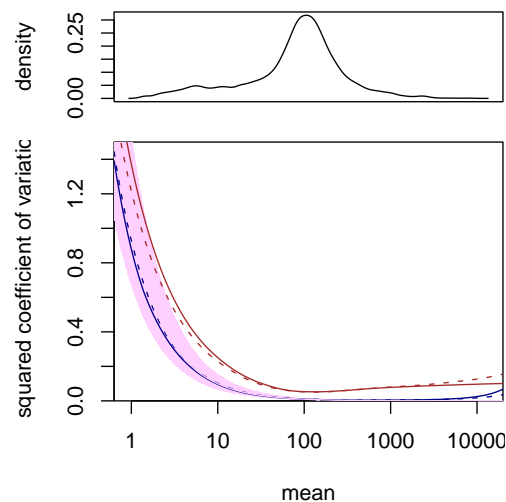


**Figure 8:** Noise estimates for the data of Nagalakshmi et al. (2008). The data allow assessment of technical variability (between library preparations from aliquots of the same yeast culture) and biological variability (between two independently grown cultures). The blue curves depict the squared coefficient of variation at the common scale,  $w_\rho(q)/q^2$  (see Equation (9)) for technical replicates, the red curves for biological replicates (solid lines, *dT* data set, dashed lines, *RH* data set). The data density is shown by the black curve in the top panel. The purple area marks the range of the shot noise for the range of library sizes in the data set. One can see that the noise between technical replicates follows closely the shot noise limit, while the noise between biological replicates exceeds shot noise already for low count values.

would be inadequate.

For the Poisson approximation, a key paper is the work by Marioni et al. (2008), who studied the *technical* reproducibility of RNA-Seq. They extracted total RNA from two tissue samples, one from the liver and one from the kidneys of the same individual. From each RNA sample they took seven aliquots, prepared a library from each aliquot according to the protocol recommended by Illumina and sampled each library on one lane of a Solexa genome analyzer. For each gene, they then calculated the variance of the seven counts from the same tissue sample and found very good agreement with the variance predicted by a Poisson model. In line with our arguments in Section 2, Poisson shot noise is the minimum amount of variation to expect in a counting process. Thus, Marioni et al. (2008) concluded that the technical reproducibility of RNA-Seq is excellent, and that the variation between technical replicates is close to the shot noise limit.

From this vantage point, Marioni et al. (2008) suggested to use the Poisson model (and Fisher's exact test, or a likelihood ratio test as an approximation to it) to test whether a gene is differentially expressed between their two samples. It is now vital to notice that



a rejection from such a test only informs us that the difference between the average counts in the two samples is larger than one would expect between *technical* replicates. Hence, we do not know whether this difference is due to the different tissue type, kidney instead of liver, or whether a difference of the same magnitude could have been found as well if one had compared two samples from different parts of the same liver, or from livers of two individuals.

Figure 1 shows that shot noise (purple region) is only dominant for very low count values, while already for moderate counts, the effect of the biological variation between samples exceeds the shot noise by many orders of magnitude. This is confirmed by comparison of technical with biological replicates (Nagalakshmi et al., 2008). In Figure 8, we used *DESeq* to obtain variance estimates for the data of Nagalakshmi et al. (2008). The analysis indicates that the difference between technical replicates barely exceeds shot noise level, while biological replicates differ much more.

Tests for differential abundance that are based on a Poisson model, such as proposed by Jiang and Wong (2009) or Wang et al. (2010) should thus be interpreted with caution, as they will tend to underestimate the effect of biological variability.

Consequently, it is preferable to use a model that allows for overdispersion. While for the Poisson distributions, variance and mean are equal, the negative binomial distributions are a generalisation that allow for the variance to be larger. The most advanced of the published methods using this family of distributions is likely *edgeR* (Robinson and Smyth, 2007). *DESeq* owes its basic idea to a good part to *edgeR*, but differs in several aspects.

## 5.2 Sharing of information between genes

First, we discovered that the use of total read counts as estimates of sequencing depth, and hence for the adjustment of observed counts between samples (as recommended by Robinson and Smyth (2007) and other authors) may result in high apparent differences between replicates, and hence in poor power to detect true differences. *DESeq* uses the more robust size estimate Equation (5); in fact, *edgeR*'s power increases when it is supplied with those size estimates instead.

For small numbers of replicates such as often encountered in practice, it is not possible to obtain simultaneously reliable estimates of the variance and mean parameters of the NB distribution. *edgeR* addresses this problem by estimating a single *common dispersion* parameter. In our method, we make use of the possibility to estimate a more flexible, mean-

dependent local regression. The amount of data available in typical experiments is large enough to allow for sufficiently precise local estimation of the dispersion. Over the large dynamic range that is typical for RNA-Seq, the raw SCV often appears to change noticeably, and taking this into account allows *DESeq* to avoid bias towards certain areas of the dynamic range in its differential-expression calls (see Figures 3 and 4).

This flexibility is the most substantial difference between *DESeq* and *edgeR*, as simulations show that *edgeR* and *DESeq* perform comparably if provided with artificial data with constant SCV (Supplementary Note F). *edgeR* attempts to make up for the rigidity of the single-parameter noise model by allowing for an adjustment of the model-based variance estimate with the per-gene empirical variance. An empirical Bayes procedure, which was originally developed for the *limma* package (Smyth, 2004), determines how to combine these two sources of information optimally. However, for typically low replicate numbers, this so-called tagwise dispersion mode seems to rather reduce *edgeR*'s power (Section 4.4).

Third, we have suggested a simple and robust way of estimating the raw variance from the data. Robinson and Smyth (2008) employed a technique they called quantile-adjusted conditional maximum likelihood to find an unbiased estimate for the raw SCV. The *quantile adjustment* refers to a rank-based procedure that modifies the data such that the data seem to stem from samples of equal library size. In *DESeq*, differing library sizes are simply addressed by linear scaling (Equations (2) and (3)), suggesting that quantile adjustment is an unnecessary complication. The price we pay for this is that we need to make the approximation that the sum of NB variables in Equation (10) be itself NB distributed. While it seems that neither the quantile adjustment nor our approximation pose reason for concern in practice, *DESeq* is conceptionally simpler and computationally faster.

Our approach provides useful diagnostics. Plots such as Supplementary Figure S2 are helpful to judge the reliability of the tests. In Figures 1b and 8, it is easy to see at which mean value biological variability dominates over shot noise; this information is valuable to decide whether the sequencing depth or the number of biological replicates is the limiting factor for detection power, and so helps in planning experiments. A heatmap as in Figure 6 is useful as data quality control.

## 6 The R package *DESeq*

We implemented our method as a package for the statistical environment R (R Development Core Team,

2009). As input, it expects a table of count data. The data, as well as metadata, such as sample classes, are managed with the S4 class *CountDataSet*, which is derived from *eSet*, Bioconductor’s standard data type for table-like data. The package provides high-level functions to perform analyses such as in Section 4 with only a few commands, allowing researchers with little knowledge of R to use it. This is demonstrated with examples in the documentation (the so-called package vignette). Furthermore, lower-level functions are supplied for more experienced users who wish to deviate from the standard work flow. A typical calculation, such as the analysis shown in Section 4.2, takes a few minutes of computation time on a desktop computer.

## Acknowledgements

We are grateful to Paul Bertone for sharing the neural stem cells data and to Julien Gagneur for helpful comments on the manuscript. S.An. has been partially funded by the European Union Research and Training Network “Chromatin Plasticity”.

## References

- Agresti, A. (2002). *Categorical Data Analysis*. Wiley, 2nd edition.
- Benjamini, Y. and Hochberg, Y. (1995). Controlling the false discovery rate: a practical and powerful approach to multiple testing. *J. Roy. Stat. Soc. B*, 57, 289.
- Bliss, C. I. and Fisher, R. A. (1953). Fitting the negative binomial distribution to biological data. *Biometrics*, 176–200.
- Cameron, A. C. and Trivedi, P. K. (1998). *Regression analysis of count data*. Cambridge University Press.
- Clark, S. J. and Perry, J. N. (1989). Estimation of the negative binomial parameter  $\kappa$  by maximum quasi-likelihood. *Biometrics*, 45, 309.
- Engström, P. et al. (2010). Transcriptional characterization of glioblastoma stem cell lines using tag sequencing. In preparation. [Full author list: P. Engström, D. Tommei, S. Stricker, A. Smith, S. Pollard, P. Bertone].
- Jiang, H. and Wong, W. H. (2009). Statistical inferences for isoform expression in RNA-Seq. *Bioinformatics*, 1026, 1026.
- Lawless, J. F. (1987). Negative binomial and mixed poisson regression. *The Canadian Journal of Statistics*, 15, 209.
- Licatalosi, D. D. et al. (2008). HITS-CLIP yields genome-wide insights into brain alternative RNA processing. *Nature*, 456, 464.
- Loader, C. (1999). *Local Regression and Likelihood*. Springer.
- Loader, C. (2000). Fast and accurate computation of binomial probabilities. <http://projects.scipy.org/scipy/raw-attachment/ticket/620/loader2000Fast.pdf> (Note: This is a copy of the original paper, which is no longer available online.).
- Loader, C. (2007). *locfit: Local Regression, Likelihood and Density Estimation*. R package version 1.5-4.
- Marioni, J. C. et al. (2008). RNA-seq: An assessment of technical reproducibility and comparison with gene expression arrays. *Genome Res.*, 18, 1509.
- McCullagh, P. and Nelder, J. A. (1989). *Generalized Linear Models*. Chapman & Hall/CRC, 2nd edition.
- Morrissy, A. S. et al. (2009). Next-generation tag sequencing for cancer gene expression profiling. *Genome Research*, 19, 1825.
- Mortazavi, A. et al. (2008). Mapping and quantifying mammalian transcriptomes by RNA-Seq. *Nature Methods*, 5, 621.
- Nagalakshmi, U. et al. (2008). The transcriptional landscape of the yeast genome defined by RNA sequencing. *Science*, 320, 1344.
- R Development Core Team (2009). *R: A Language and Environment for Statistical Computing*. R Foundation for Statistical Computing, Vienna, Austria. ISBN 3-900051-07-0.
- Robertson, G. et al. (2007). Genome-wide profiles of STAT1 DNA association using chromatin immunoprecipitation and massively parallel sequencing. *Nat. Meth.*, 4, 651 .
- Robinson, M. D., McCarthy, D. J. and Smyth, G. K. (2010). edgeR: a Bioconductor package for differential expression analysis of digital gene expression data. *Bioinf.*, 26, 139.
- Robinson, M. D. and Smyth, G. K. (2007). Moderated statistical tests for assessing differences in tag abundance. *Bioinformatics*, 23, 2881.
- Robinson, M. D. and Smyth, G. K. (2008). Small-sample estimation of negative binomial dispersion, with applications to SAGE data. *Biostat*, 9, 321.
- Saha, K. and Paul, S. (2005). Bias-corrected maximum likelihood estimator of the negative binomial dispersion parameter. *Biometrics*, 61, 179.
- Smith, A. M. et al. (2009). Quantitative phenotyping via deep barcode sequencing. *Genome Research*, 19, 1836.
- Smyth, G. K. (2004). Linear models and empirical bayes methods for assessing differential expression in microarray experiments. *Stat. Appl. Gen. Mol. Biol.*, 3. Article 3.
- Wang, L. et al. (2010). DEGseq: an R package for identifying differentially expressed genes from RNA-seq data. *Bioinformatics*, 26, 136.
- Whitaker, L. (1914). On the Poisson law of small numbers. *Biometrika*, 10, 36.

[Supplement on following pages.]

## Supplementary Notes

### A Parameterization of the negative binomial distribution

An integer valued random variable  $K$  is said to follow a negative binomial distribution with parameters  $p \in ]0, 1[$  and  $r \in ]0, \infty[$  if (Cameron and Trivedi, 1998)

$$\Pr(K = k) = \binom{k+r-1}{r-1} p^r (1-p)^k. \quad (16)$$

This two-parametric distribution can, equivalently, be parametrised in terms of its mean  $\mu$  and variance  $\sigma^2$ , via

$$p = \frac{\mu}{\sigma^2} \quad \text{and} \quad r = \frac{\mu^2}{\sigma^2 - \mu}. \quad (17)$$

### B Variance estimator

In Section 2.2, we claim that  $\hat{w}_{i\rho} - z_{i\rho}$ , as defined in Eqs. (7, 8), is an unbiased estimator for the raw variance  $v_{i\rho}$ . To show this, we compute the expectation value of  $\hat{w}_{i\rho}$ . To simplify notation, we suppress the indices  $i$  and  $\rho$  in the following. Furthermore, we neglect differences between the true library sizes  $s_j$  and their estimates  $\hat{s}_j$ . Then,

$$\hat{Q} = \frac{1}{m} \sum_{j=1}^m \frac{K_j}{s_j}$$

is an unbiased estimator of  $q$ , because, due to Equation (2),  $\mathbb{E} K_j = s_j q_0$ . Next, we examine

$$(m-1) \hat{w} = \sum_{j: \rho_j = \rho} \left( \frac{k_j}{s_j} - \hat{q} \right)^2.$$

Taking expectations on both sides yields

$$(m-1) \mathbb{E} \hat{w} = \left( 1 - \frac{1}{m} \right) \sum_j \frac{\mathbb{E} K_j^2}{s_j^2} - \frac{1}{m} \sum_{\substack{j,l \\ j \neq l}} \frac{\mathbb{E} K_j K_l}{s_j s_l}$$

For  $j \neq l$ ,  $K_j$  and  $K_l$  are independent, and hence  $\mathbb{E} K_j K_l = s_j s_l q^2$ , while for  $j = l$ , we have  $\mathbb{E} K_j^2 = (\mathbb{E} K_j)^2 + \text{Var} K_j = s_j^2 q^2 + s_j q + s_j^2 v$  by the definition of variance and Equation (3). Using this, we find

$$\mathbb{E} \hat{w} = v + \underbrace{\frac{\hat{q}}{m} \sum_j \frac{1}{s_j}}_{z}$$

where the underbraced part is the bias correction term  $z$ .

### C Removal of bias due to reparametrization

When estimating distribution parameters for the purpose of calculating  $p$  values from the distribution, bias in the parameter estimates can cause problems. As the choice of parameters to characterize a distribution is arbitrary, the question arises for which set of parameters bias should be minimized in order to then allow for accurate inference.

For the NB distribution, we investigated this issue: By means of simulations with similar settings as in Supplementary Note F, we found that if we used the unbiased mean and variance estimates  $\hat{q}_{i\rho}$  and  $w_\rho(\hat{q}_{i\rho})$  from Equations (6) and (9) to calculate  $p$  values with Equation (11) for simulated data without any differential expression, the  $p$  values were not uniform, but tended to be too small when the number of replicates was low. In previous work on inference based on the NB distribution, the authors usually aimed at getting unbiased estimates for another pair of parameters, namely for the mean and either for the dispersion parameter (e.g., Bliss and Fisher (1953)) or, more recently, for its reciprocal, i.e., the quantity we denote the raw SCV (e.g., Clark and Perry (1989); Lawless (1987); Saha and Paul (2005)). The question why this parameter pair is suitable is discussed by Lawless (1987). Our simulations support that approach: if we calculate the raw SCV from the mean and variance estimates, reparametrize to mean and raw SCV remove the bias that this reparametrization introduced to the raw SCV (using the numerical procedure detailed below), the null  $p$  values become uniform in the simulations.

**Numerical bias removal.** Let  $f_{mq}$  be a function that maps a true raw SCV value  $\gamma$  to the expectation of the estimate  $\hat{\gamma} = (\hat{\sigma}^2 - \hat{\mu})/\hat{\mu}^2$ .  $f_{mq}(\gamma)$  approaches its limit for  $q \rightarrow \infty$  very fast; the changes for  $q \gtrsim 30$  are negligible for our purposes, and the values for small  $q$  only lead to a conservative overestimation of the variance. Hence, we precalculate  $f_{mq}$  for a fixed,

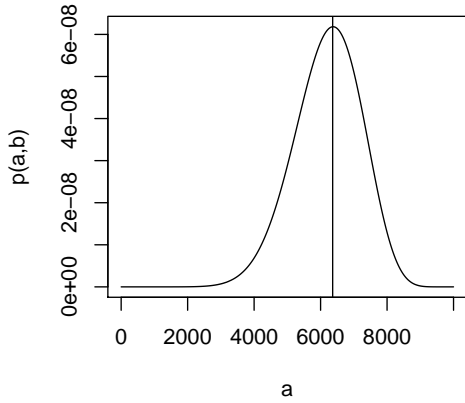


**Figure S1:** Shape of the function  $p(a, b)$ , with  $k_S = 10,000$ ,  $b = k_{AB} - a$ ,  $\mu_A = 7,000$ ,  $\mu_B = 4,000$ ,  $\sigma_A^2 = \mu_A + 0.1\mu_A^2$  and  $\sigma_B^2 = \mu_B + 0.1\mu_B^2$ . The vertical line marks the estimate  $k_S\mu_A/(\mu_A + \mu_B)$  for the mode.

large value of  $q$ , and all the values  $m = 2, 3, \dots, 15$ , at a grid of values for  $\gamma$ , invert it and interpolate in order to bias-correct an estimate  $\hat{\gamma}$ . For  $m \gtrsim 15$ ,  $f_{mq}$  is sufficiently close to the identity function to make a bias correction unnecessary for our purposes.

## D Numerical calculation of the p values

Evaluating the sums in Equation (11) requires some care. In HTS data, the count sum  $k_S$  can be large (e.g., millions of counts for a single strongly expressed gene), and calculating all the summands individually may take a long time and result in rounding error accumulation. Figure S1 shows the dependence of  $p(a, b)$  (as defined in Section 3 and using Equation (14) for the distribution of  $K_A$ ) on  $a$  for typical parameters. The function is unimodal, with mode approximately at ratio  $a/b$  equal to the ratio of the means of  $K_A$  and  $K_B$ . The function's simple shape allows the following numerical approximation: start at evaluating the sum from the peak (or rather, from its estimated location according to the means) and proceed outwards in two passes, first left, then right. During the summation, watch the changes of the value and keep adapting the step size according to a pre-defined precision goal. The value of  $p$  for the actually observed count values  $k_A$  and  $k_B$  is calculated beforehand, so that both the sum in the numerator and denominator of Equation (11) can be calculated in the same pass. To compute the density the NB distribution, we use a function (Loader,

**Residuals ECDF plot for condition 'GNS'**

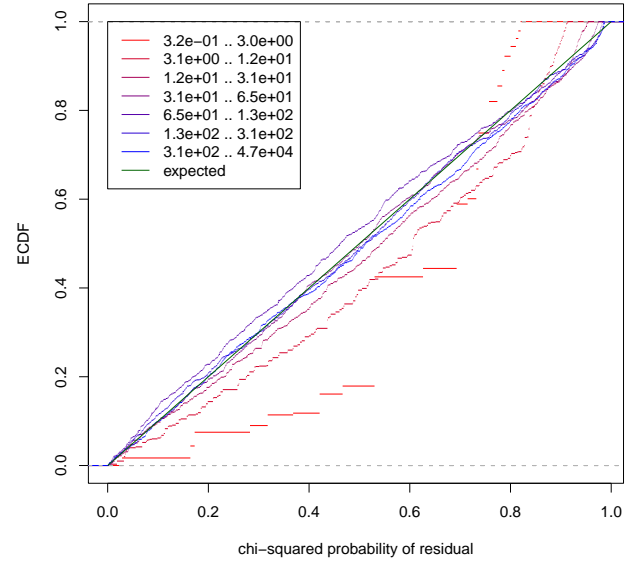


**Figure S2:** Empirical cumulative density function (ECDF) plots for the  $\chi^2$ -probabilities of the residuals from the variance fit (orange line in Figure 1), stratified by the mean. The green line is the diagonal, which is the expected curve if the residuals follow the  $\chi^2$  distribution with  $m_\rho - 1 = 1$  degree of freedom.

2000) in the C API of R (R Development Core Team, 2009).

## E Diagnostics for the local regression

The choice of the gamma family for the local regression can be motivated as follows: If the size-adjusted counts  $k_{ij}/s_j$  in the sample variance estimate  $w_{i\rho}$  calculated in Equation (7) were normally distributed with true variance  $\sigma_{ij}^2$ , the quantity  $(m_\rho - 1)w_{i\rho}/\sigma_{ij}^2$  would follow a  $\chi^2$  distribution with  $m_\rho - 1$  degrees of freedom, and this should hold as well for the residuals,

$$\xi_{i\rho} = (m_\rho - 1) \frac{w_{i\rho}}{w(\hat{q}_{i\rho})}$$

(where we have replaced the true variance  $\sigma^2$  with its fitted value  $w(\hat{q}_{i\rho})$ ). Even though the size-adjusted counts are not normally distributed, this is still a useful approximation for GLM local regression. Among the exponential families commonly used with generalized linear models, the gamma family, which includes the  $\chi^2$  distributions, is close to the actual distribution of the residuals, and since generalized linear models tend to show robustness against misspecification, we expect a reasonable fit. In order to verify this, we

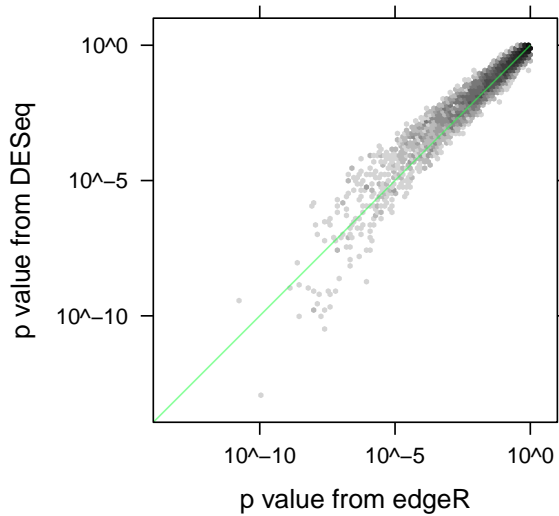
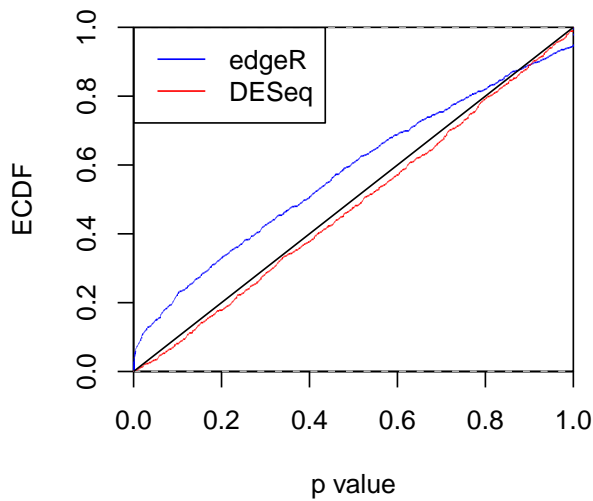


**Figure S3:** Results from a simulation mimicking the distribution of counts in the neural stem cell data. (a) Uniformity of the  $p$  values calculated for the genes that were not differentially expressed, shown with an ECDF plot. (b) Comparison of the  $p$  values between the *DESeq* and *edgeR* for the genes that were simulated as differentially expressed.

can check how well the residuals  $\xi_{i\rho}$  follow a  $\chi^2$  distribution. To this end, we calculate the  $\chi^2$  quantiles of the  $\xi_{i\rho}$  and check them for uniformity by plotting their empirical cumulative density function (ECDF). Figure S2 shows the ECDF curves for the condition  $\rho = \text{GNS}$ , stratified by the estimated means  $\hat{q}_{i\rho}$ . As one can see, the residuals follow the distribution reasonably well. Only for extremely low counts (below 5), the fitting quality is reduced. At such low counts, the shot noise dominates (see Figure 1b), and inaccuracies in the estimation of the raw noise are no reason for concern.

It is worth noting that the  $\chi^2$  distribution for  $m_{\text{GNS}} - 1 = 1$  degree of freedom has a heavy right tail. Hence, the fact that in Figure 1 so many points lie far above the fitted line does not imply a bad fit.

## F Simulations

As a check of the correctness of *DESeq* and to further explore its performance in comparison to *edgeR*, we performed simulations. Here, we show a set of typical results for simulation parameters chosen to resemble the situation in the neural stem cell data set.

We drew true mean values  $q_i$  for 20,000 genes from an exponential distribution with rate  $1/250$ . Each gene was considered “truly differentially expressed” (tDE) with probability 30%, and for all tDE genes

a  $\log_2$  fold change was randomly drawn from a normal distribution with mean 0 and standard deviation 2.5. Finally, four count values were drawn for each gene, two for condition A and two for condition B, from negative binomial distributions, with the given means and variances as below, and multiplied by the size factors, which we chose as 0.5, 1.7, 1.4 and 0.9, similar to those seen in experimental data

For the variances, we catered to *edgeR*’s assumption and set the raw SCV to a constant, 0.5. Then, we used both our approach and *edgeR* to test for differential expression. *edgeR* was given the true size factors, while our approach had to estimate them from the data. In this setting, *edgeR* (running in common-dispersion mode) correctly estimated the raw SCV with good accuracy. Both approaches controlled the type-I error rate correctly: the percentage of type-I errors at 5% nominal significance level was (averaged over 10 simulation runs) 3.1% for *DESeq* and 3.4% for *edgeR*. (See Figure S3a for a plot with data from one run). At 10% FDR, *DESeq* discovered 21% of the truly differentially expressed genes, and *edgeR* found 26%. Finally, both methods stayed below the nominal 10% FDR with an actual FDR of 5.1% (*DESeq*) and 6.9% (*edgeR*). Note that *edgeR*’s apparent slight advantage is to be expected here as the simulation stipulates a constant raw SCV.